On The Design of Planar Microwave Components Using Multilayer Structures

Wolfgang Schwab, *Member, IEEE*, and Wolfgang Menzel, *Senior Member, IEEE*

Abstract—The design of planar microwave components using multilayer configurations with potentially arbitrary numbers of dielectric layers and metallization planes is described. Analysis and design are based on a combination of a spectral domain immittance matrix approach and standard CAD methods. To verify the design procedure, three examples—a microstrip-slot-line-microstrip transition, a stripline band-pass filter, and a microstrip coupler with lines on different sides of a common ground plane—are investigated theoretically and experimentally.

Fig. 1. Some examples of single and multiplane discontinuities.

I. INTRODUCTION

PLANAR transmission lines like microstrip, coplanar line, finline, or suspended stripline find widespread applications in hybrid and monolithic integrated microwave and millimeter wave circuit. Consequently, a lot of work has been spent on analyzing transmission line parameters, discontinuities, e.g., [1], [2], and designing complete passive and active circuits, e.g. [3]-[5].

An increasing system complexity leads to new challenges in circuit design, too. One way to cope with this is the combination of different types of transmission lines to achieve optimal performance. An early example for this is the finline balanced mixer [6], [7], which combines finline, coplanar line and microstrip, forming a compact broadband component; a later example is the technique of uniplanar MMIC's, consisting of coplanar and slot lines [8]. Another way of dealing with complex microwave circuits are three dimensional or multilayer components. Possible applications are high density interconnects for very high speed digital circuits [9], [10], complex microwave front ends combining MMIC chips and carrier substrates including circuit elements with excessive area requirements (compared to a suitable MMIC chip size), or circuits arranged on both sides of a common ground plane with interconnects between the layers.

Circuits of this kind may comprise several layers of dielectric and metallizations, different substrate materials, and different types of transmission lines, and generally, there is some kind of electromagnetic coupling between structures in the same or different layers ([10]-[16]).

In general, full wave methods have to be employed to characterize circuits of this kind. For example, integral
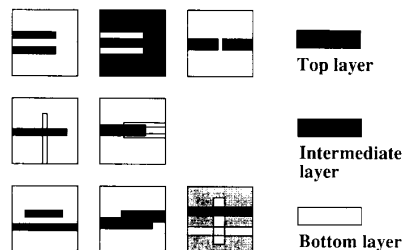
equation technique and transverse resonance technique have been applied to some types of transition between different substrate planes [17]-[22].

In this paper, analysis and design of nonradiating passive multilayer components is described; similar design methods can be applied to circuits including active devices. For a good design efficiency, field theoretical methods are combined with conventional transmission line and CAD calculations. For the analysis of the critical parts of the circuits, a spectral domain immittance matrix approach for an arbitrary number of substrate layers and conductor planes is used combined with resonance methods; in this way, a great number of single- and multi-level discontinuities can be analysed, some of which are shown in Fig. 1. To test this method, a double transition between microstrip, slotline, and microstrip again is investigated as a compact, complex structure. In combination with standard band-pass filter design, a suspended stripline filter with resonators in different planes was designed, and finally, a coupler between microstrip lines on different sides of a ground plane was calculated using both full wave methods and transmission line theory.

II. CALCULATION METHOD FOR MULTIPLANE DISCONTINUITIES

The calculation method used here is based on a two dimensional spectral domain immittance approach for shielded resonant structures [23], [24] with N conductor planes and n dielectric layers.

The Fourier transform of all field quantities is given by

$$\tilde{\psi}(\alpha, \beta) = \int_{-\infty}^{+\infty} \int_{-\infty}^{+\infty} \psi(x, z)$$

$$\cdot \exp\left[j \cdot (\alpha \cdot x + \beta \cdot z) \right] dx\ dz.$$

Because of the shielding side walls (dimensions a and c), α and β take discrete values

$$\alpha = \frac{m \cdot \pi}{a},$$

$$\beta = \frac{n \cdot \pi}{c}, \qquad n, m = 0, \pm 1, \pm 2, \pm 3, \cdots .$$

The inverse Fourier transform

$$\psi(x, z) = \frac{1}{(2 \cdot \pi)^2} \cdot \int_{-\infty}^{+\infty} \int_{-\infty}^{+\infty} \tilde{\psi}(\alpha, \beta)$$

$$\cdot \exp\left[-j \cdot (\alpha \cdot x + \beta \cdot z)\right] d\alpha \, d\beta$$

illustrates that all field components can be interpreted as superpositions of inhomogeneous waves propagating in v-direction as shown in Fig. 2(a). For each angle Θ, waves can be decomposed into a TM-to-y wave $(\tilde{E}_y, \tilde{E}_v, \tilde{H}_u)$ and a TE-to-y wave $(\tilde{H}_y, \tilde{E}_u, \tilde{H}_v)$. The metallization in each conductor plane is represented by surface current densities $\tilde{J}_{ui}$ and $\tilde{J}_{vi}$, where each $\tilde{J}_{ui}$ creates TE fields and each $\tilde{J}_{vi}$ TM fields only. The dependence of the electromagnetic field perpendicular to the substrate plane is described by equivalent transmission line circuits for the TE and TM waves with the propagation constants

$$\gamma_i = \sqrt{\alpha^2 + \beta^2 - k_0^2 \cdot \epsilon_{ri}}$$

and wave admittances

$$\tilde{Y}_{0i}^h = \frac{\gamma_i}{j \cdot \omega \cdot \mu_0}, \qquad \tilde{Y}_{0i}^e = \frac{j \cdot \omega \cdot \epsilon_0 \cdot \epsilon_{ri}}{\gamma_i}$$

for all n dielectric layers (Fig. 2(b)). In these transmission line circuits, every current source $\tilde{J}_{ui}$ and $\tilde{J}_{vi}$ represents the surface current density on the conductor in the ith conductor-plane. Each current source $\tilde{J}_{ui}$ and $\tilde{J}_{vi}$ creates electric fields $\tilde{E}_u$ and $\tilde{E}_v$ in all N conductor planes. Accordingly, the TE and TM tangential electric fields in all N conductor planes include contributions of all TE and TM current sources, respectively. This dependence is described in the impedance matrix equations

$$\tilde{E}_{ui} = \tilde{Z}_{i1}^h \tilde{J}_{u1} + \cdots + \tilde{Z}_{ii}^h \tilde{J}_{ui} + \cdots + \tilde{Z}_{iN}^h \tilde{J}_{uN}$$

$$\tilde{E}_{vi} = \tilde{Z}_{i1}^e \tilde{J}_{v1} + \cdots + \tilde{Z}_{ii}^e \tilde{J}_{vi} + \cdots + \tilde{Z}_{iN}^e \tilde{J}_{vN}.$$

The TE and TM electric fields at one conductor plane are related to the TE and TM current sources of the same conductor plane by the TE and TM input impedances $\tilde{Z}_{ii}^h$ and $\tilde{Z}_{ii}^e$. The relation between TE and TM current sources and electric fields in different planes is given by the TE and TM transfer impedances $\tilde{Z}_{ij}^h$ and $\tilde{Z}_{ij}^e$. The input impedances $\tilde{Z}_{\mu\mu}^h$ and $\tilde{Z}_{\mu\mu}^e$ are impedances looking into the equivalent transmission line circuits at the μth conductor plane lying between the mth and $(m + 1)$th dielectric layer and hence are expressed as

$$\tilde{Z}_{\mu\mu}^h = \frac{1}{\tilde{Y}_{u\mu\mu}^h + \tilde{Y}_{d\mu\mu}^h}, \qquad \tilde{Z}_{\mu\mu}^e = \frac{1}{\tilde{Y}_{u\mu\mu}^e + \tilde{Y}_{d\mu\mu}^e},$$
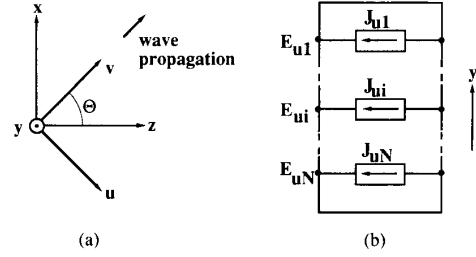

Fig. 2. (a) Coordinate systems. (b) TE equivalent transmission line circuit for the spectral domain immitance matrix approach.

where $\tilde{Y}_{u\mu\mu}$ and $\tilde{Y}_{d\mu\mu}$ are admittances looking up and down into the corresponding circuit at the μth conductor plane. They are calculated successively by transforming the short circuits represented by the upper and lower shielding through all dielectric layers above and below the μth conductor plane, respectively, using transmission line theory.

The transfer impedances $\tilde{Z}_{\mu\nu}$ connect the current sources of the νth conductor plane to the tangential electric field of the μth conductor plane,

$$\tilde{Z}_{\mu\nu} = \tilde{Z}_{\nu\nu} \prod_{i=q}^{p} \frac{\tilde{Y}_{0i}/\sinh \gamma_i h_i}{\tilde{Y}_{ui-1} + \tilde{Y}_{0i} \coth \gamma_i h_i},$$

where p is the number of the dielectric layer below the μth conductor plane and q is the number of the dielectric layer above the νth conductor plane.

The resulting immitance matrix equations for TE and TM waves are transformed from the (u, v)-coordinate system block to the (x, z)-coordinate system.

Related to the following solution procedure, the analysis given above is especially advantageous for layers with metallic strips; for layers with slots, the equation should be solved for the current density, e.g.,

$$\tilde{J}_i = \sum_j \tilde{Y}_{ij} \cdot \tilde{E}_j.$$

For structures where layers with strips and slots are mixed, this leads to a hybrid representation. As an example, the equations for a structure with one strip and one slot plane are given by

$$\begin{pmatrix} \tilde{E}_{x1} \\ \tilde{E}_{z1} \\ \tilde{J}_{x2} \\ \tilde{J}_{z2} \end{pmatrix} = \begin{pmatrix} \tilde{Z}_{xx11} & \tilde{Z}_{xz11} & \tilde{T}_{xx12} & \tilde{T}_{xz12} \\ \tilde{Z}_{zx11} & \tilde{Z}_{zz11} & \tilde{T}_{zx12} & \tilde{T}_{zz12} \\ \tilde{T}_{xx21} & \tilde{T}_{xz21} & \tilde{Y}_{xx22} & \tilde{Y}_{xz22} \\ \tilde{T}_{zx21} & \tilde{T}_{zz21} & \tilde{Y}_{zx22} & \tilde{Y}_{zz22} \end{pmatrix} \begin{pmatrix} \tilde{J}_{x1} \\ \tilde{J}_{z1} \\ \tilde{E}_{x2} \\ \tilde{E}_{z2} \end{pmatrix}.$$

The unknown current densities and electrical slot fields (and their Fourier transforms) on the right side of the immitance matrix equations are expanded in terms of suitable basis functions $\tilde{e}_i, \tilde{j}_i$ as presented in [1] including suitable edge terms. Applying Galerkin's procedure and Parseval's theorem result in a homogeneous eigenvalue matrix equation for the amplitude coefficients of current

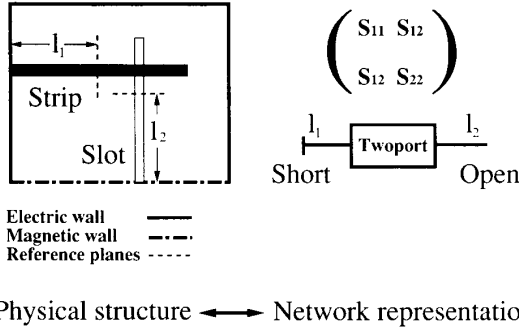Physical structure ◄──► Network representation

Fig. 3. Physical structure and equivalent network representation of a microstrip-slotline transition as a resonance configuration.

densities and electrical fields represented by the vector $\vec{c}$:

$$\sum_{j=1}^{P} \left\{ \sum_{\alpha} \sum_{\beta} \begin{Bmatrix} \tilde{e}_i \\ \tilde{j}_i \end{Bmatrix} \cdot \begin{Bmatrix} \tilde{T}_{ij} \\ \tilde{Y}_{ij} \\ \tilde{Z}_{ij} \end{Bmatrix} \cdot \begin{Bmatrix} \tilde{e}_j \\ \tilde{j}_i \end{Bmatrix} \right\} \cdot c_j = 0,$$

$$i = 1, 2, \cdots, P,$$

where P is the number of expansion functions.

Nontrivial solutions (resonance conditions) are obtained by varying relevant resonator dimensions for a fixed frequency until the matrix determinant becomes zero.

From these resonance calculations the scattering matrix of multiplane discontinuities can be derived. This is demonstrated for a microstrip-slotline transition in Fig. 3. Each resonance calculated as described above is set equal to a corresponding network representation as shown on the right side of Fig. 3. As the S-matrix in this (reciprocal) network contains three complex unknown quantities, three sets of resonance conditions, i.e., three pairs of different lengths l_1 and l_2 have to be computed to solve for the unknown S-parameters [1]. For symmetric structures, the computational effort can be reduced considerably including this *a priori* information into the computation process.

The computer program based on the procedure described above was set up very generally as far as the Green's functions (spectral domain impedances and admittances) and the solution process are concerned. In this way, a wide variety of multiplane structures can be analyzed simply by defining the relevant expansion functions.

Extensive convergence investigation have been done in relation to the number of basis functions as well as the number of the discrete values of the Fourier variables α and β which have to be taken into account for the summation in the Galerkin's procedure. As an example for a relative big structure, convergence behaviour of S_{11} for a single microstrip-slotline transition is presented in Fig. 4.

Computation time for one frequency point ranges from one to several minutes on a high-end workstation, depending on the size and the complexity of the structure.
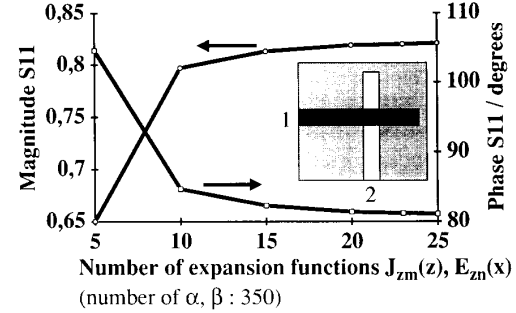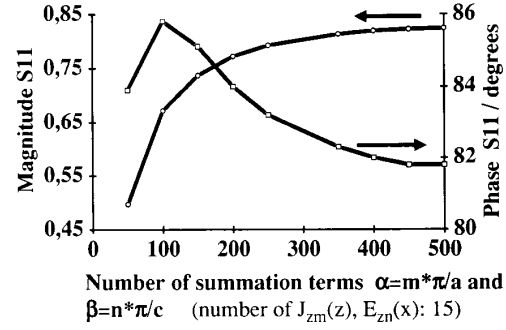

Number of summation terms $\alpha=m*\pi/a$ and $\beta=n*\pi/c$ (number of $J_{zm}(z)$, $E_{zn}(x)$: 15)

Number of expansion functions $J_{zm}(z)$, $E_{zn}(x)$
(number of α, β : 350)

Fig. 4. Convergence behavior of S_{11} of a microstrip-slotline transition (Substrate thickness 0.635 mm, ϵ_r = 10, stripwidth 0.57 mm, slot width 0.05 mm, dimensions of the shielding box 25 mm * 25 mm * 60 mm, f = 8 GHz).

III. ANALYSIS AND DESIGN OF MULTIPLANE COMPONENTS

Since even the analysis of "simple" discontinuities using accurate field theoretical methods requires a considerable amount of computation time, the design, i.e., the optimization of components with several discontinuities at a number of frequencies, would demand too much time. On the other hand, simple but accurate models (like equivalent circuits) are not available for many types of discontinuities like multiplane transitions.

One possibility to reduce these problems is the combination of field theoretical methods with classical network synthesis or CAD methods based on simple network and transmission line theory whenever possible. In this context, the influence of coupling of adjacent circuit elements by stray fields, surface waves, radiation, or higher order modes has to be weighted against required accuracy as well as tolerances of semiconductor parameters, fabrication processes, and measurement accuracy.

Furthermore, the S-parameters of small discontinuities normally vary slowly with frequency, so for narrowband applications, one computation at the center frequency may be sufficient, and for wider band applications, values calculated only at a few frequency points can be interpolated with good accuracy.

In the following, three examples for multiplane components are presented: a microstrip-slotline-microstrip transition, a suspended stripline bandpass filter and a slot
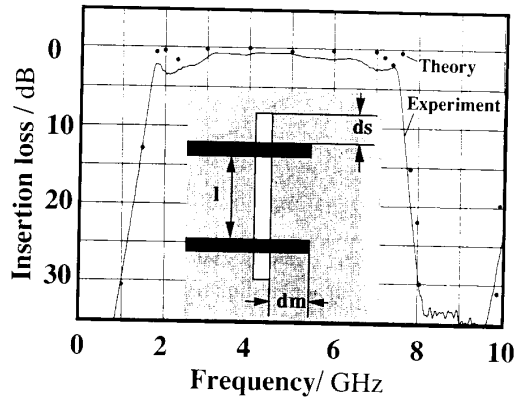
Fig. 5. Measured and calculated transmission coefficient of a microstrip-slot-microstrip transition (ϵ_r = 11.1 (RT/Duroid 6010), h = 1.27 mm, s = 0.53 mm, w = 1.0 mm, l = 20.4 mm, d_m = 5.24 mm, d_s = 6.65 mm).

coupler between two microstrip lines situated on both sides of a common ground plane.

The first example, a microstrip-slotline-microstrip transition, was chosen to test the calculation procedure described in Section II for a relatively complex structure. Fig. 5 shows the configuration with its dimensions. The measured transmission coefficient between port 1 and 2 is compared with calculated values. The calculation was made for the complete configuration, taking into account the symmetry of the structure.

The design of a suspended substrate stripline filter (Fig. 6(a)) was based on the equivalent circuit of capacitively coupled transmission line resonators (Fig. 6(b)). The transmission line dimensions and the capacitances can be calculated from standard filter design tables (e.g., [25]). In the suspended substrate line configuration, the capacitances are formed by the coupled ends of strip resonators placed on different sides of the substrate. In contrast to end or side coupled resonators on one side of the substrate, a very wide range of coupling coefficients are possible depending on the distance or the overlapping of the two lines on different substrate sides, giving the chance to design filters with wider bandwidths, too.

In the case of the example presented here, the S-parameters of this transition from one side of the substrate to the other were calculated as a function of the overlapping at the center frequency of the filter. This dependence for the transmission coefficient S_{21} is shown in Fig. 7 (For the filter design, only a few points of this curve are necessary). The curve of Fig. 7 was calculated at 12 different points and interpolated with cubic spline functions. From this chart, the gap dimensions can be chosen according to the required transmission coefficient calculated from the related capacitance of the equivalent circuit. For the lengths of the resonators, corrections have to be made in relation to the phase of S_{21} of the real planar structure.

A filter for 10 GHz with 400 MHz bandwidth was designed and fabricated in this way. Due to an increased underetching and a small shift between front and back side structure, a slight frequency shift and unsymmetry was found in the experimental filter response; the unsymme-
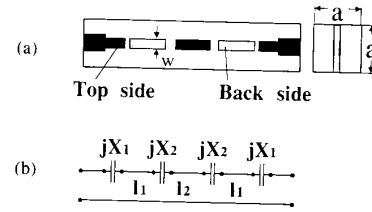

Fig. 6. Stripline filter. (a) Stripline configuration of a three resonator bandpass filter. (b) Network representation.
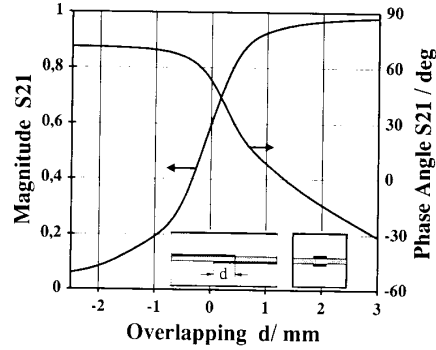

Fig. 7. Calculated magnitude and phase of a single stripline gap junction as a function of overlapping d(ϵ_r = 2.2, (RT/Duroid 5880), h = 0.254 mm, w = 1.75 mm, a = 5.0 mm).
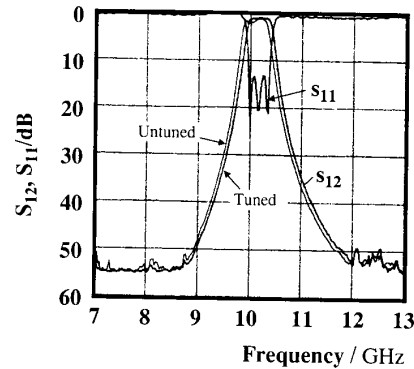

Fig. 8. Measured reflection and transmission coefficients of the tuned and untuned suspended stripline filter.

try, however, could be removed easily with some light tuning (Fig. 8). The insertion loss of the filter was 0.8 dB.

The last example is a coupling structure between two microstrip lines on different sides of a common ground plane. The coupling occurs through slots in the ground plane. Couplers of this kind with different coupling slot configurations have already been investigated with approximate calculations, e.g., [14], [15]. The coupling structure presented here consists of four square slots in the common ground plane between the two microstrip lines as shown in Fig. 9(a). In a first step, the four port scattering parameters of the structure with one square slot only were calculated at a number of frequency points using the spectral domain method as described above. These
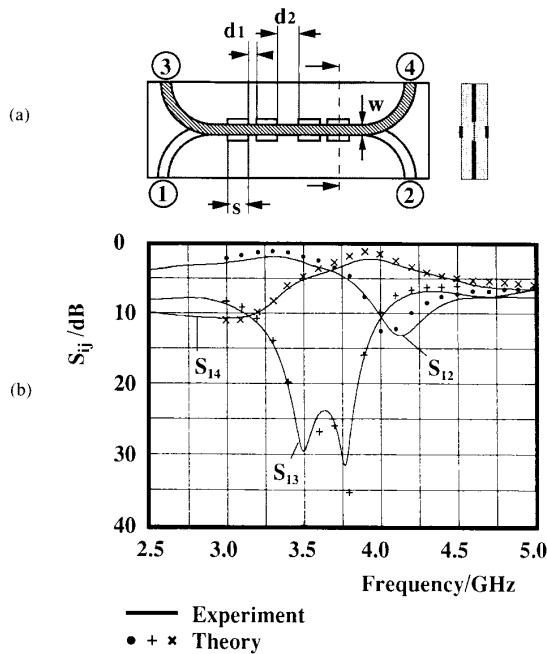
Fig. 9. Microstrip coupler. (a) Configuration. (b) Measured and calculated transmission, coupling and isolation (ϵ_r = 2.2 (RT/Duroid 5880), h = 1.58 mm, w = 4.6 mm, s = 10.0 mm, d_1 = 2.22 mm, d_2, 12.51 mm).

S-matrix values were fed into a commercial microwave CAD program [26]. Using this CAD package, the four slot coupler was optimized as a network of four single slot structures connected by microstrip lines. The resulting dimensions are given in Fig. 9(a). Since this simple network representation does not take into account coupling between the slots—especially for the slots situated close together—the resulting complete structure was analysed with the spectral domain method in order to check this influence. Slight differences between the network and the full wave analysis were found concerning bandwidth, the overall performance, however, was maintained. Fig. 9(b) shows the measured results for transmission, coupling and directivity of the coupler in comparison to the results of the spectral domain method. In a similar way as for this example, couplers with an arbitrary number of slots with different dimensions can be designed and analyzed.

IV. CONCLUSION

Field theoretically calculations for shielded multiplane discontinuities combined with standard transmission line representations and CAD methods were used to design microwave components including several layers of dielectric and metallization. This technique leads to an acceptable computational effort compared to many methods based on rigorous computation for the complete structure.

Applying some microwave experiences, and taking into account the required accuracy and the inevitable tolerances of semiconductor elements, of fabrication processes, and of measurements, this technique leads to excellent results as can be seen from the three examples

presented in this paper. In this first step, only passive components have been investigated; in the same way, however, active components including semiconductor elements can be designed, too.

REFERENCES

[1] T. Itoh, Ed., *Numerical Techniques for Microwave and Millimeter-Wave Passive Structures*. New York: Wiley, 1989.

[2] R. Sorrentino, Ed., *Numerical Methods for Passive Microwave and Millimeter Wave Structures*, IEEE Press, 1989.

[3] *IEEE Microwave and Millimeter-Wave Monolithic Circuits Symp. Dig.*, 1990.

[4] T. H. Oxley and C. Burnett, "mm-Wave (30–110 GHz) hybrid microstrip technology," *Microwave J.*, Part I, Mar. 1986, pp. 36–44, Part II, May 1986, pp. 177–185.

[5] P. J. Meier and H. J. Kuno, "Integrated finline: The second decade," *Microwave J.*, Part I, Nov. 1985, pp. 31–54, Part II, Dec. 1985, pp. 30–46.

[6] V. H. Gysel, "A 26.5 to 40 GHz planar balanced mixer," in *Proc. 5th European Microwave Conf.*, 1975, pp. 491–495.

[7] W. Menzel and H. Callsen, "Integrated fin-line components and subsystems at 60 and 94 GHz," *IEEE Trans. Microwave Theory Tech.*, vol. MTT-31, pp. 142–146, Feb. 1983.

[8] T. Hirota et al., "Uniplanar MMIC hybrids-A proposed new MMIC structure," *IEEE Trans. Microwave Theory Tech.*, vol. MTT-35, pp. 576–581, June 1987.

[9] G. L. Holz, "Firing process improves high-density packaging," *Microwaves & RF*, pp. 122–128, Nov. 1990.

[10] L. Carin and K. J. Webb, "Isolation effects in single- and dual- plane VLSI interconnects," *IEEE Trans. Microwave Theory Tech.*, vol. 38, pp. 396–404, Apr. 1990.

[11] J. B. Knorr, "Slot Line Transitions," *IEEE Trans. Microwave Theory Tech.*, vol. 22, pp. 548–554, May 1974.

[12] J. J. Burke and R. W. Jackson, "Surface-to-surface transition via electromagnetic coupling of microstrip and coplanar waveguide," *IEEE Trans. Microwave Theory Tech.*, vol. 37, pp. 519–525, Mar. 1989.

[13] I. E. Lösch and J. A. G. Malherbe, "Design procedure for inhomogeneous coupled line sections," *IEEE Trans. Microwave Theory Tech.*, vol. 36, pp. 1186–1190, July 1988.

[14] T. Tanaky et al., "Slot-coupled directional couplers between double-sided substrate microstrip lines and their applications," *IEEE Trans. Microwave Theory Tech.*, vol. 36, pp. 1752–1757, Dec. 1988.

[15] G. V. Jogiraju and V. M. Pandharipande, "Stripline to microstrip line aperture coupler," *IEEE Trans. Microwave Theory Tech.*, vol. 38, pp. 440–443, Apr. 1990.

[16] M. Aikawa and H. Ogawa, "Double-sided MIC's and their applications," *IEEE Trans. Microwave Theory Tech.*, vol. 37, pp. 406–413, Feb. 1989.

[17] H. Y. Yang and N. G. Alexópoulos, "A dynamic model for microstrip-slotline transition and related structures," *IEEE Trans. Microwave Theory Tech.*, vol. 36, pp. 286–293, Feb. 1988.

[18] ——, "Basic blocks for high-frequency interconnects: Theory and experiment," *IEEE Trans. Microwave Theory Tech.*, vol. 36, pp. 1258–1264, Aug. 1988.

[19] H. Y. Yang et al., "Design of transversely fed EMC microstrip dipole arrays including mutal coupling," *IEEE Trans. Microwave Theory Tech.*, vol. 38, pp. 145–151, Feb. 1990.

[20] T. S. Horng et al., "A full-wave analysis of shielded microstrip line-to-line transition," in *1990 IEEE MTT-S Int. Symp. Dig.*, pp. 251–254.

[21] N. L. Van den Berg and P. B. Katehi, "Full-wave analysis of aperture coupled shielded microstrip lines," in *1990 IEEE MTT-S Int. Symp. Dig.*, pp. 163–166.

[22] T. Uwano et al., "Characterization of microstrip-to-slotline transition discontinuities by transverse resonance analysis," *Alta Frequenza*, vol. LVII-N.5, pp. 183–191, June 1988.

[23] T. Itoh, "Analysis of microstrip resonators," *IEEE Trans. Microwave Theory Tech.*, vol. MTT-22, pp. 946–952, Nov. 1974.

[24] ——, "Spectral-domain immitance approach for dispersion characteristics of generalized printed transmission lines," *IEEE Trans. Microwave Theory Tech.*, vol. MTT-28, pp. 733–736, July 1980.

[25] G. Matthaei, L. Young, and E. M. T. Jones, *Microwave Filters, Impedance-Matching Networks, And Coupling Structures*. Norwood, MA: Artech House, 1980.

[26] *OCTOPUS User Manual,* ARGUMENS Mikrowellenelektronik GmbH, Duisburg, 1990.

Wolfgang Schwab (M'88) was born on October 12, 1961, in Munich, Germany. He received the Dipl.-Ing. degree in electrical engineering from the Technical University of Munich in 1986.

From 1986 to 1989 he was with AEG Radio and Radar System Group (now Telefunken Systemtechnik), Ulm, Germany, working on MMIC design problems. Since 1989 he has been with the Department of Engineering Sciences, Microwave Technique, at the University of Ulm.

Wolfgang Menzel (M'89–SM'90) was born in Brilon-Wald, Germany, on December 10, 1948. He received the Dipl.-Ing. degree from the Technical University of Achen, Germany, in 1974, and the Dr.-Ing. degree from the University of Duisburg, Germany, in 1977.

From 1974–1979 he was with the University of Duisburg working on microstrip circuit problems. In 1979 he joined AEG-Telefunken (now Telefunken Systemtechnik), where he became head of the mm-Wave-Department in 1984. In August 1989 he was appointed to a full professorship at the University of Ulm. His current research interests are microwave and mm-wave integrated circuits and systems.